

The dependence of α -tocopheroxyl radical reduction by hydroxy-2,3-diaryl-xanthenes on structure and micro-environmentPatrice Morlière,^{*a,b,c} Larry K. Patterson,^{c,d} Clementina M. M. Santos,^{e,f} Artur M. S. Silva,^e Jean-Claude Mazière,^{a,b,c} Paulo Filipe,^g Ana Gomes,^h Eduarda Fernandes,^h M. Beatriz Q. Garcia^h and René Santus^{c,i}

Received 21st September 2011, Accepted 8th December 2011

DOI: 10.1039/c2ob06612b

The flavonoid quercetin is known to reduce the α -tocopheroxyl radical (\cdot TocO) and reconstitute α -tocopherol (TocOH). Structurally related polyphenolic compounds, hydroxy-2,3-diaryl-xanthenes (XH), exhibit antioxidant activity which exceeds that of quercetin in biological systems. In the present study repair of \cdot TocO by a series of these XH has been evaluated using pulse radiolysis. It has been shown that, among the studied XH, only 2,3-bis(3,4-dihydroxyphenyl)-9H-xanthen-9-one (XH9) reduces \cdot TocO, though repair depends strongly on the micro-environment. In cationic cetyltrimethylammonium bromide (CTAB) micelles, 30% of \cdot TocO radicals are repaired at a rate constant of $\sim 7.4 \times 10^6 \text{ M}^{-1} \text{ s}^{-1}$ by XH9 compared to $1.7 \times 10^7 \text{ M}^{-1} \text{ s}^{-1}$ by ascorbate. Water-soluble Trolox (TrOH) radicals (\cdot TrO) are restored by XH9 in CTAB (rate constant $\sim 3 \times 10^4 \text{ M}^{-1} \text{ s}^{-1}$) but not in neutral TX100 micelles where only 15% of \cdot TocO are repaired (rate constant $\sim 4.5 \times 10^5 \text{ M}^{-1} \text{ s}^{-1}$). In basic aqueous solutions \cdot TrO is readily reduced by deprotonated XH9 species leading to ionized XH9 radical species (radical $\text{p}K_{\text{a}} \sim 10$). An equilibrium is observed ($K = 130$) yielding an estimate of 130 mV for the reduction potential of the [\cdot X9,H⁺/XH9] couple at pH 11, lower than the 250 mV for the [\cdot TrO,H⁺/TrOH] couple. A comparable value (100 mV) has been determined by cyclic voltammetry measurements.

Introduction

Xanthenes are natural heterocyclic compounds present in significant quantities in numerous plant species, especially those of the *Guttiferae* and *Gentianaceae* families.¹ In addition to their anti-allergenic, anti-inflammatory and antitumor properties,² a strong antioxidant activity has been demonstrated for these natural

products.³ Such activity is ascribed to the presence of hydroxyl groups and/or a catechol moiety at key molecular sites. Synthetic hydroxylated 2,3-diaryl-xanthenes⁴ have been shown to readily scavenge various reactive oxygen and nitrogen species ($\cdot\text{O}_2^-$, HOCl, $\cdot\text{NO}$, ONOO⁻ and $^1\text{O}_2$).⁵ Members of this family (XH: see Table 1 for structures) may bear up to 4 hydroxyl groups at various sites on the two aryl rings, and the dependence of

^aNSERM U1088, Laboratoire de Biochimie, CHU Amiens - Hôpital Nord, place Victor Pauchet, F-80054 Amiens Cedex 1, France.

E-mail: morliere.patrice@chu-amiens.fr; Fax: +33 3 22 66 85 93; Tel: +33 3 22 66 86 69

^bUniversité de Picardie Jules Verne, Faculté de Médecine et de Pharmacie, EA 4292, F-80036 Amiens, France

^cCHU Amiens, Laboratoire de Biochimie, F-80054 Amiens, France

^dUniversity of Notre Dame, Radiation Laboratory, Notre Dame, Indiana 46556, USA

^eUniversity of Aveiro, Department of Chemistry & QOPNA, 3810-193 Aveiro, Portugal

^fPolytechnic Institute of Bragança, School of Agriculture, Department of Vegetal Production and Technology, 5301-855 Bragança, Portugal

^gUniversidade de Lisboa, Hospital de Santa Maria, Clínica

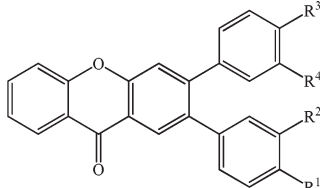
Universitária de Dermatologia, 1600 Lisbon, Portugal

^hREQUIMTE, Departamento de Ciências Químicas, Faculdade de Farmácia, Universidade do Porto, Rua Aníbal Cunha, 164, 4099-030 Porto, Portugal

ⁱMuséum National d'Histoire Naturelle, Département RDDM, F-75231 Paris, France

Table 1 Chemical structure of the hydroxy-2,3-diaryl-xanthenes (XH) used in this study

	R ¹	R ²	R ³	R ⁴
XH3	OH	OH	H	H
XH6	OH	OH	OH	H
XH7	H	H	OH	OH
XH8	OH	H	OH	OH
XH9	OH	OH	OH	OH



XH3: 2-(3,4-dihydroxyphenyl)-3-phenyl-9H-xanthen-9-one, XH6: 2-(3,4-dihydroxyphenyl)-3-(4-hydroxyphenyl)-9H-xanthen-9-one, XH7: 3-(3,4-dihydroxyphenyl)-2-phenyl-9H-xanthen-9-one, XH8: 3-(3,4-dihydroxyphenyl)-2-(4-hydroxyphenyl)-9H-xanthen-9-one, XH9: 2,3-bis(3,4-dihydroxyphenyl)-9H-xanthen-9-one.

antioxidant activity on these structural features has been characterized by fast spectroscopic techniques.⁶ In addition to this structure–activity relationship, it has been observed in model biological systems that the combination of hydrophobicity and steric factors also governs the antioxidant effectiveness of these molecules.⁶ For example, while XH9 is the least effective member of this series in the inhibition of Cu^{2+} -induced lipid peroxidation in human low density lipoproteins (LDL), it is the most efficient scavenger of O_2^- and halogenated peroxy radicals in aqueous micellar systems. Owing to its four hydroxyl groups, XH9 may be expected to locate preferentially in LDL towards the surface of the water-rich outer layer comprised of phospholipids, cholesterol and ApoB-100 apolipoprotein. By contrast, the more hydrophobic XH bearing two OH (XH3 and XH7) or three OH (XH6 and XH8) are most effective against LDL lipid peroxidation and they are expected to distribute more deeply into the phospholipid layer where the labile hydrogen sites participating in peroxidative chain reactions are found.⁶

In human plasma, LDL is an important carrier of α -tocopherol (vitamin E, TocOH). It acts as an essential lipophilic chain-breaking antioxidant, which protects cell membranes against lipid peroxidation by reducing lipid peroxy radicals with concomitant formation of $\cdot\text{TocO}$ radicals. In living cells, TocOH is only a minor membrane component but its effectiveness as an antioxidant is thought to be greatly enhanced through the repair/recycling of $\cdot\text{TocO}$ by other cellular antioxidants, such as ascorbate or glutathione.⁷ However, it has also been proposed that supplementation with natural antioxidants such as flavonoids could complement this recycling mechanism. In this regard, it has been shown that the flavone quercetin, a highly potent natural antioxidant, can restore TocOH *in vitro* by reducing the $\cdot\text{TocO}$ radical.⁸ Because hydroxy-2,3-diarylxanthenes are as good as—or better antioxidants than—quercetin, it is of considerable interest to examine with this molecular group the possibility of a similar “restorative effect” on vitamin E consumption. Electron transfer reactions from XH (the hydrogen donor) to the $\cdot\text{TocO}$ radical (the acceptor) have been studied here by fast spectroscopic techniques. As these molecules are all rather hydrophobic, such reactions have been investigated, at neutral pH, in model multiphase aqueous media. Additionally, these multiphase systems mimic some of the micro-environmental complexity inherent to biological structures. The present investigation has thus been carried out in buffered (pH 7) solutions of cationic cetyltrimethylammonium bromide (CTAB) micelles and—for the purpose of comparison—in buffered solutions of uncharged Triton X100 (TX100) micelles. Pulse radiolysis was employed, as it is particularly apt for measuring electron transfer kinetics. With this technique one may convert all primary radical species produced by water radiolysis into oxidizing $\cdot\text{Br}_2^-$ radical-anions or $\cdot\text{N}_3$ radicals. These then react readily with TocOH or its water soluble analogue, Trolox C (TrOH). A parallel investigation was also carried out in basic media where the hydroxy-2,3-diarylxanthenes become more soluble with ionization. Furthermore, in homogeneous aqueous phase, non-equilibrium concentrations of antioxidant radicals in the presence of another hydrogen donor can be obtained with the fast response pulse radiolysis method. The kinetics of relaxation of the system to equilibrium can be followed, from which thermodynamic parameters such as the reduction potential can be estimated.⁹ α -Tocopherol is insoluble

in water. Consequently, electron transfer has also been characterised using the water-soluble analogue TrOH, since it is believed that the corresponding radical ($\cdot\text{TrO}$) has the same reduction potential as $\cdot\text{TocO}$ ($E_0^{\circ} [\cdot\text{TocO},\text{H}^+/\text{TocOH}] \sim 480$ mV).⁸ Furthermore, the use of micellar systems differing in size, viscosity, nature of their water interface and electrostatic charge allows useful insight into micro-environmental effects on the repair reaction. It is shown here that XH9, bearing four OH substituents, can repair radicals formed from either TrOH or TocOH while other members of the XH family do not. Further, because of the role played by ascorbate (AH^-) *in vivo* in extending TocOH activity ($E_0^{\circ} [\cdot\text{A}^-,\text{H}^+/\text{AH}^-] \sim 280$ mV) it has been used as a reference allowing direct thermodynamic comparison of α -tocopheroxyl radical repair by XH9 and AH^- , occurring under similar experimental conditions.

Materials and methods

Chemicals and routine equipment

The five hydroxylated 2,3-diarylxanthenes (Table 1) have been synthesized as described by Santos *et al.*⁴ and their formula names have been abbreviated here in the same manner as in the preceding article from our laboratories.⁶ All other chemicals were of analytical grade and were used as received from the suppliers. Cetyltrimethylammonium bromide, ascorbic acid and TocOH were purchased from Sigma (St Louis, Mo, USA). Spectroscopic grade dimethylsulfoxide and TX100 were supplied by Merck (Darmstadt, Germany). The phosphate buffer (pH 7) was prepared in pure water obtained with a reverse osmosis system from Ser-A-Pure Co. The water from this system exhibited a resistivity of >18 Mohms cm^{-1} and a total organic content of <10 ppb. Pure N_2O was used for pulse radiolysis experiments. Absorption spectrophotometry was carried out in quartz cells with Uvikon 922 and Shimadzu UV-2101PC spectrophotometers.

Cyclic voltammetry

Five mM XH9 or XH3 were dissolved in DMSO and further diluted to a final concentration 0.1 mM in the supporting electrolytes. To cover the pH range, the following buffers have been used: 0.2 M sodium phosphate buffer (pH 7.4), 0.2 M acetate buffer (pH 4) and 0.1 M carbonate-bicarbonate buffer (pH 11). Electrochemical measurements were carried out in an Autolab electrochemical system (Eco Chemie model PGSAT 10) and data were acquired using GPES software (version 4.9). Voltammetric signals were recorded at room temperature. The working electrode was a glassy carbon electrode (3.0 mm) whereas an Ag/AgCl (KCl 3 mol L^{-1}) electrode and a carbon electrode were used as reference and auxiliary electrodes, respectively. Before each experiment, the glassy carbon working electrode was polished with a 0.075 μm alumina aqueous slurry. Cyclic voltammograms were obtained with a single cycle performed at a scan rate of 100 mV s^{-1} .

Pulse radiolysis

Pulse radiolysis measurements were performed with the Notre Dame Radiation Laboratory 8-MeV linear accelerator, which

generates 5 ns pulses of up to 30 Gy. In general, the doses used here were 10–15 Gy. The detection system previously described^{10,11} allows one to follow reaction kinetics up to 2 ms after the radiolytic pulse in the 320–700 nm spectral range. For the study of slow reactions up to 0.5 s, the pulsed xenon lamp was replaced by a LedEngin LCZ 40 watt LED emitting in the wavelength range 420–750 nm. Radical concentrations calculated from transient absorbance data are referenced to ${}^{\cdot}(\text{SCN})_2^-$ dosimetry. The extinction coefficient for ${}^{\cdot}(\text{SCN})_2^-$ is $7580 \pm 60 \text{ M}^{-1} \text{ cm}^{-1}$ at 472 nm, and the radiolytic yield (G value) for ${}^{\cdot}\text{OH}$ in N_2O -saturated solution has been measured as $\sim 0.63 \mu\text{M Gy}^{-1}$ (or $\sim 0.63 \mu\text{M kg J}^{-1}$).¹² To conserve XH solution, a microcell (optical path: 1 cm, i.d: 2 mm and volume 120 μL) was used for transient recording. Numerical integrations, carried out in analyses of some rate data, were conducted using the Scientist software from Micromath Scientific Software.

Preparation of the antioxidant solutions

Solutions for pulse radiolysis at neutral pH were prepared in 10 mM, pH 7, phosphate buffer containing 10 mM CTAB or 0.3% TX100 to which were added aliquots of 0.4 M stock solutions of XH in dimethylsulfoxide. In measurements with CTAB, the solution temperature was maintained at 25 °C to avoid crystallisation of CTAB in the optical quartz cell and associated Teflon[®] tubing. For the determination of the pK_a of the one-electron oxidation product of XH9, the aqueous solutions of the antioxidants were thoroughly and continuously degassed until pulse radiolysis measurements were made to avoid auto-oxidation. The pH of solutions containing the various antioxidants was adjusted below pH 9 with phosphate buffers and above pH 9 with aliquots of 0.01 M to 1 M NaOH just before undergoing pulse radiolysis.

Determination of the pK_a

The determination of the pK_a for the mono- and di-anionic XH9 equilibrium was carried out with 50 μM XH9 dissolved in 10 mM aqueous 2-amino-2-methyl-1-propanol (AMP) ($\text{pK}_a = 9.7$). In the pH range 8.5–10.85, pH was adjusted by addition of HCl. Between pH 6.9 and pH 7.6 the 10 mM AMP solution was prepared in 50 mM phosphate buffer and pH was also adjusted with HCl. Above pH 11, pH was adjusted with NaOH added to 10 mM AMP solution. At high pH, 50 μM XH9 were prepared just before absorption measurements at 420 nm also to avoid any auto-oxidation.

Results and discussion

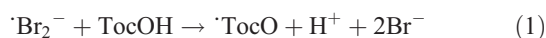
Studies in micellar solutions

While insoluble in pH 7 buffer, TocOH is readily soluble at concentrations up to 1 mM in CTAB or TX100 micellar solutions. The distribution of such hydrophobic molecules in micelles is best described by Poisson statistics. Under our experimental conditions, the CTAB and TX100 micelle concentrations ($[\text{M}]$) are found to be 70 μM and 30 μM , respectively.¹³ The fraction $f(i)$ of micelles with i TocOH molecules is given by $f(i) = (Q^i/i!) \times \exp(-Q)$ with $Q = [\text{TocOH}]/[\text{M}]$. With 1 mM TocOH, the

calculation shows that more than 99.99% of CTAB and TX100 micelles contain at least one TocOH.

Electron transfer reactions in CTAB micelles

In the presence of 0.1 M KBr in the N_2O -saturated CTAB solutions, ${}^{\cdot}\text{OH}$ radicals are formed directly during water radiolysis and by conversion of hydrated electrons to ${}^{\cdot}\text{OH}$ with N_2O . These are then transformed into strongly oxidizing ${}^{\cdot}\text{Br}_2^-$ radical-anions (yield of $\sim 0.64 \mu\text{M Gy}^{-1}$) which are subsequently trapped by the positively charged CTAB micelles within less than 10 ns. With the ${}^{\cdot}\text{Br}_2^-$ concentration produced by a dose of 10 Gy, the only significant fraction of CTAB micelles containing ${}^{\cdot}\text{Br}_2^-$ is $f(1) = 0.08$.¹³ It may be assumed that pseudo-first order kinetics apply here to the formation of ${}^{\cdot}\text{TocO}$. In CTAB micelles, the absorption maximum of the ${}^{\cdot}\text{TocO}$ transient lies at 430 nm and ${}^{\cdot}\text{TocO}$ radical generation by the reaction



is essentially completed within 12 μs (data not shown), save for a very small long term growth which occurs over 10–20 msec. From the pseudo first order growth observed for the principal portion of the reaction in the presence of 1 mM TocOH, an apparent bimolecular reaction rate constant of $\sim 1.5 \times 10^8 \text{ M}^{-1} \text{ s}^{-1}$ for reaction (1) can be estimated. A ${}^{\cdot}\text{TocO}$ yield of $\sim 0.4 \mu\text{M Gy}^{-1}$ can be determined in this micellar solution assuming a molar extinction coefficient of $7100 \text{ M}^{-1} \text{ cm}^{-1}$ comparable to that of the ${}^{\cdot}\text{TrO}$ radical¹⁴ at this wavelength in buffer. The ${}^{\cdot}\text{TocO}$ transient absorption in this system may be seen to not decay over the first 50 ms following radiolysis (Fig. 1A).

In order to determine whether a repair of the ${}^{\cdot}\text{TocO}$ radical is possible using XH, the XH9 derivative was chosen first since XH9 has been shown to be the most potent antioxidant of the hydroxy-2,3-diarylxanthone family in our previous studies, with regard to its radical scavenging ability.^{5,6} Because of its limited solubility in neutral aqueous solutions, XH9 readily incorporates into the micelles. As can be seen in Fig. 1A, addition of XH9 leading to a concentration of 200 μM in the TocOH solution markedly accelerates the 430 nm transient decay of the ${}^{\cdot}\text{TocO}$ radical. Simultaneously, as illustrated in Fig. 1B, the weak transient absorbance observed with TocOH alone at 550 nm is superseded by a stronger absorbance growing over ~ 10 ms. This behaviour is attributable to production of the ${}^{\cdot}\text{X9}$ radical, known to absorb significantly at 550 nm.⁶ Fig. 1B also shows the long lived absorbance of the ${}^{\cdot}\text{X9}$ radical observed with 200 μM XH9 alone. It is likely that the slow absorbance growth observed over 10 ms with both the ${}^{\cdot}\text{TocO}$ and ${}^{\cdot}\text{X9}$ radicals is due to migration of the radicals in a part of the micelle with different polarity as a result of the electron distribution changes and solvation sphere modification after ${}^{\cdot}\text{Br}_2^-$ oxidation. A rather short residence time for ${}^{\cdot}\text{Br}_2^-$ on CTAB micelles as reported in the literature makes it unlikely that this slow step is due to some slow oxidation process.¹⁵ Taken together, these observations are consistent with an electron transfer reaction:



It is admitted that electron transfer and H-atom transfer are the two main mechanisms by which reduction of radical species by polyhydroxylated antioxidants can occur. The H-atom transfer is

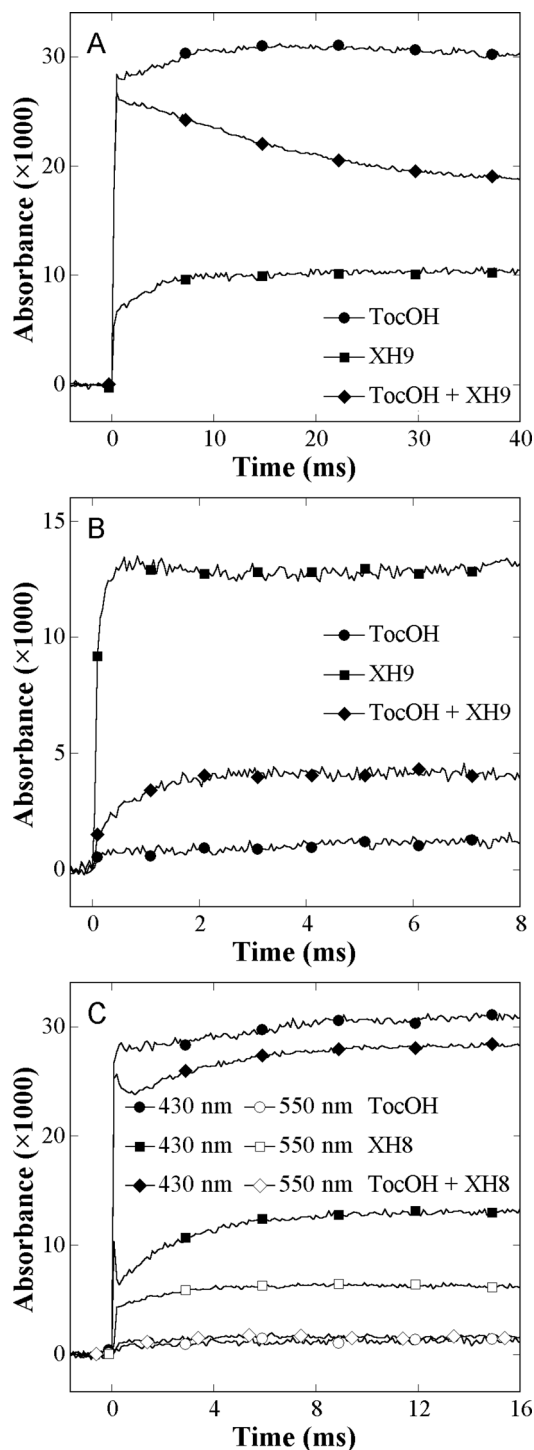


Fig. 1 A. Time dependence of 430 nm transient absorbance after pulse radiolysis of N_2O -saturated, 10 mM phosphate buffer (pH 7) containing 10 mM CTAB and 0.1 M KBr as well as: (●) 1 mM TocOH; (■) 200 μM XH9; (◆) 1 mM TocOH + 200 μM XH9. Dose was 14.4 Gy. B. Same conditions as in Fig. 1 A but absorbance measurements have been carried out at 550 nm. C. Time dependence of transient absorbance at 430 nm (closed symbols) and 550 nm (open symbols) after pulse radiolysis of N_2O -saturated, 10 mM phosphate buffer (pH 7) containing 10 mM CTAB and 0.1 M KBr and (●,○) 1 mM TocOH; (■,□) 200 μM XH8; (◆,◇) 1 mM TocOH + 200 μM XH8; note at early times a small contribution of $\text{X}8$ species to the kinetics at 430 nm due to the competitive reaction of Br_2^- with TocOH and XH8. Dose was 14 Gy.

a one-step process whereas the electron transfer occurs *via* formation of the substrate radical-cation which rapidly deprotonates. In both cases, the same net result is observed. Here it is important to note that study on the repair of α -tocopheroxyl radicals has been carried out in positively charged CTAB micelles. Contrary to several other studies carried out at steady state in homogenous organic solutions,¹⁶ our experiments were carried out in highly dielectric aqueous micellar solutions. Due to their negative charge, all Br_2^- radicals are trapped within a few ns in the water-rich Stern layer of the CTAB micelles where protons are also available. Then, the reaction: $\text{Br}_2^- + \text{TocOH} \rightarrow \text{TocO} + 2 \text{Br}^- + \text{H}^+$ occurs within about 10 μs with the substrate. It is generally admitted that in many instances the appearance of a product (characterized by an absorption spectrum) corresponding to a net loss of electron strongly supports the occurrence of an electron transfer reaction here followed by a proton exchange as a primary process. Alternatively, in other cases, a product corresponding to a net loss of hydrogen atom is formed (for example in the case of the XH oxidation by O_2^- radicals⁶) leading to the same species as their oxidation with Br_2^- radicals (see Ref. 6) and the occurrence of an electron transfer may be less obvious. Here, we believe that the strong electrostatic field at the water-micelle interface would favour a stepwise electron transfer followed by a proton transfer (ET-PT) rather than a hydrogen atom transfer whose rate constant depends on the homolytic OH bond dissociation enthalpy of the antioxidant.¹⁷

From the initial TocO yield obtained with Fig. 1A data and the data from Fig. 1B, the electron transfer efficiency can be estimated to be $\sim 30\%$. With the doses used in these experiments (~ 14 Gy), the TocO radical concentration in the micellar solution is about $\sim 4 \mu\text{M}$. Thus, with a XH9 concentration of at least 50 μM , conditions for pseudo first order reactions are fulfilled. The pseudo first order plot, shown in Fig. 2, has been

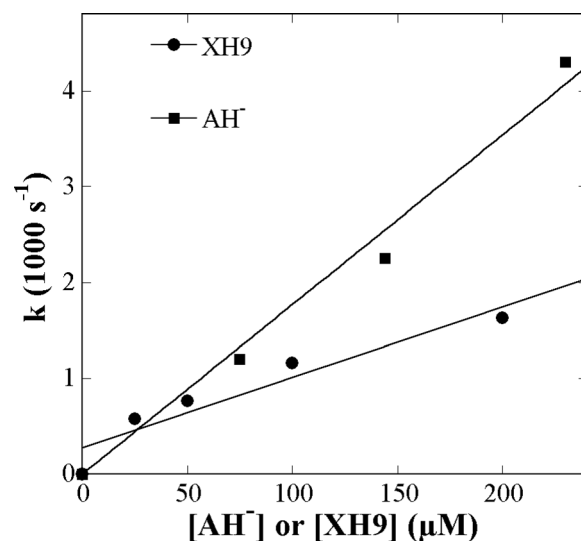


Fig. 2 Plots giving the dependence of the rate constant for $\text{X}9$ transient growth at 550 nm on the XH9 concentration (●) and the dependence of the TocO decay rate constant at 430 nm on the ascorbate (AH^- , ■) concentration. Pulse radiolysis measurements were carried out in N_2O saturated, 10 mM phosphate buffer (pH 7) containing 10 mM CTAB, 0.1 M KBr and 1 mM TocOH in the presence of XH9 or ascorbate. Dose was 14.4 Gy.

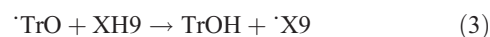
constructed from growth of the $\cdot\text{X9}$ radical transient absorbance at 550 nm as a function of XH9 concentration. A second order rate constant of $\sim 7.4 \times 10^6 \text{ M}^{-1} \text{ s}^{-1}$ for reaction (2) is found. This rate constant determination has been carried out at 550 nm because $\cdot\text{TocO}$ dominates the time-dependent absorbance at 430 nm. However, the contribution of a slow $\cdot\text{X9}$ radical decay in this medium (see below) as well as the kinetics of re-localization of $\cdot\text{TocO}$ and/or $\cdot\text{X9}$ (see Fig. 1A) have been neglected in this estimate which may lead to some uncertainty in the intercept of the first order plot in Fig. 2.

Comparable measurements have been performed with the other XH derivatives included in Table 1. No evidence for an ET–PT or a hydrogen transfer reaction from these XH to the $\cdot\text{TocO}$ radical has been observed as exemplified with XH8 on Fig. 1C. Fig. 1C also suggests that the species resulting from the $\cdot\text{X8}$ transformation do not react with the $\cdot\text{TocO}$ radical. Furthermore as XH3 was the most effective XH in the protection of human LDL against the Cu^{2+} -induced lipid peroxidation, chosen as a model biological system,⁶ its cyclic voltammetry has been carried out. The reduction potential of XH3 at pH 7.4 is 340 mV (*vs* NHE) higher than that of XH9 (170 mV) but lower than that calculated for TocOH (470 mV) (see below). The lack of reactivity of the other XH with the α -tocopheroxyl radical is therefore somewhat surprising since—as exemplified with XH3—thermodynamic properties are still in favour of the $\cdot\text{TocO}$ radical repair. In our previous study we showed that, in CTAB micelles, the oxidation of XH9 by radicals with either low ($\cdot\text{O}_2^-$) or high ($\cdot\text{Trp}$ and halogenated alkylperoxyl radicals) reduction potentials was much easier than that of the other XH (see Table 1 in ref. 6). The higher hydrophobic character of the unreactive XH as compared to that of XH9 may lead to their solubilisation far from the Stern layer where the hydrophilic heads of XH9 and TocOH are probably located. In this case, and independently of the mechanism (ET–PT *vs.* hydrogen atom transfer) limiting kinetic factors contribute to their inability to repair the $\cdot\text{TocO}$ radical despite favorable thermodynamic factors. As XH9 was found to be a much weaker antioxidant than other XH in the protection of LDL oxidation it is likely that micro-environmental factors markedly contribute to the XH antioxidant properties in media with more complexity than the CTAB micelles.⁶ Along these lines, it may be noted that *trans*-resveratrol which has good antioxidant behaviour *in vivo* or in cultured cells does not recycle α -tocopherol.¹⁶

Because AH^- plays a key role as a physiological vitamin E recycling agent, it is of interest to compare the effectiveness of $\cdot\text{TocO}$ repair by XH9 and AH^- . To this end, the reaction rate constant for the electron transfer reaction from AH^- to $\cdot\text{TocO}$ has been measured in the same CTAB micro-environment and under the same experimental conditions as were used for XH9. It is likely that the water-soluble negatively charged AH^- interacts with the positively charged CTAB micelles at the water-micelle interface to produce elevated local concentrations, thus favouring the repair of the $\cdot\text{TocO}$ radical. As the $\cdot\text{A}^-$ radical absorbs negligibly at the 430 nm maximum of $\cdot\text{TocO}$ radical absorbance,¹⁴ the decay rate of $\cdot\text{TocO}$ radical as a function of AH^- concentration has been measured at this wavelength. Comparison of the slopes of the pseudo first order plots for electron transfer reaction with AH^- and XH9 (Fig. 2) indicates that the second order rate constant for repair by AH^- is 2.5 times higher than by XH9, *i.e.*

$\sim 1.7 \times 10^7 \text{ M}^{-1} \text{ s}^{-1}$. Incidentally, we observed that under similar experimental conditions, AH^- can repair the $\cdot\text{X9}$ radical. The second order rate constant for repair of the $\cdot\text{X9}$ radical by AH^- is $\sim 2 \times 10^7 \text{ M}^{-1} \text{ s}^{-1}$ similar to that obtained with the $\cdot\text{TocO}$ radical (data not shown). Assuming that the reactions proceed by rate determining electron transfer, at variance with the proton-coupled electron transfer mechanism reported for reaction of AH^- with other phenoxyl radical in homogenous organic solution,¹⁷ the rate constants suggest a lower reduction potential of AH^- as compared to that of XH9 in this system. It may be noted that this second order rate constant is four times lower than that found in cetyltrimethylammonium chloride micelles where the $\cdot\text{TocO}$ radical was produced by laser flash photolysis of TocOH.¹⁸ However in that system the detergent concentration was 4 times higher and no added electrolyte, such as the 0.1 M KBr used here, was present. Additionally, substitution of the Cl^- counterion for Br^- can effect the adsorption of AH^- to the micelle surface.¹⁹ As the characteristics of the micellar solution are a determining factor in such kinetics, comparison of rate constants for AH^- in the two micelle environments is difficult.

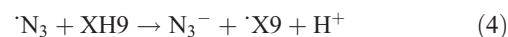
In CTAB solution, changing TocOH for TrOH, a water-soluble derivative of α -tocopherol, considerably decreases the rate constant for the ET–PT reaction:



With 2.5 mM TrOH and 200 μM XH9, this reaction extends over 200 ms, while the initial $\cdot\text{TrO}$ yield is 0.4 $\mu\text{M Gy}^{-1}$, similar to that obtained with TocOH (data not shown). Determined in the same manner as above, the second order rate constant for reaction (3) can be estimated to be $\sim 2.9 \times 10^4 \text{ M}^{-1} \text{ s}^{-1}$ including in the rate calculations, the contribution of the slow first order decay of the $\cdot\text{X9}$ radicals on this time scale. Such decay may arise from permanent product formation and/or intramolecular transformation characterised by a rate constant of 9.6 s^{-1} (data not shown). Thus, if the $\cdot\text{TrO}$ and $\cdot\text{TocO}$ radicals are assumed to have the same reduction potential,⁸ the faster ET–PT rate from XH9 to $\cdot\text{TocO}$ radical compared to that observed with $\cdot\text{TrO}$ radical is probably due to the close proximity of XH9 and TocOH within the micelle, while TrOH is supposed to be soluble in the bulk.

Electron transfer in Triton X100 micelles

In TX100 uncharged micelles, one-electron oxidation of XH9 was measured in the presence of 0.1 M NaN_3 which scavenges $\cdot\text{OH}$ radicals to produce $\cdot\text{N}_3$. The $\cdot\text{N}_3$ radicals are produced with the same radiolytic yield as $\cdot\text{Br}_2^-$ ($\sim 0.64 \mu\text{M Gy}^{-1}$) but are stronger oxidants than the latter. The transient absorbance spectrum of $\cdot\text{X9}$ species produced by the reaction:



is shown in Fig. 3. and is in good agreement with that reported previously in CTAB with $\cdot\text{Br}_2^-$ as the oxidant.⁶ However, a somewhat lower apparent molar extinction coefficient (1100 instead of 1500 $\text{M}^{-1} \text{ cm}^{-1}$ at 440 nm) is observed. This lower value is probably best explained by absent electrostatic attraction and lower residence of $\cdot\text{N}_3$ in TX100 micelles, hence allowing

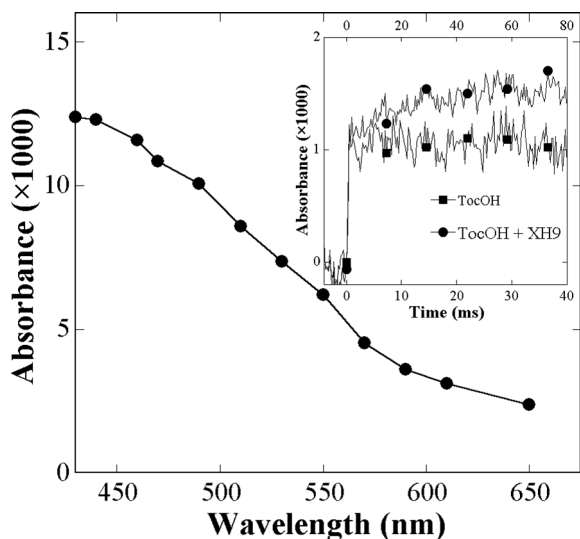


Fig. 3 Transient absorbance spectrum obtained 500 μ s after pulse radiolysis of N_2O -saturated, 10 mM phosphate buffer (pH 7) containing 0.3% TX100, 0.1 M NaN_3 and 200 μ M XH9. Dose was 18 Gy. **Insert:** Experimental conditions are the same but the solution contained 1 mM TocOH (VitE). Growth of 550 nm absorbance in the absence (■) (lower time scale) and presence (●) (upper time scale) of 200 μ M XH9. The longer time scale is used to highlight the time needed to reach a constant transient absorbance in the presence of 200 μ M XH9.

N_3 recombination to compete effectively with the electron transfer reaction (4).

The structural features of TX100 micelles have marked consequences on the repair of both \cdot TrO and \cdot TocO radicals by 200 μ M XH9. Here, no reaction has been observed with the \cdot TrO radical but some repair of the \cdot TocO radicals by XH9 is observed but at a slower rate, *i.e.* $4.5 \times 10^5 M^{-1} s^{-1}$. Further, a very low efficiency ($\sim 16\%$) is found as compared to values obtained in CTAB micelles (insert Fig. 3). It is likely that TocOH molecules are preferentially distributed in the hydrophobic core of TX100 micelles as opposed to XH9 which—because of its 4 hydroxyl substituents—should reside in the thick palisade layer (25 nm).

As a result of the high palisade layer viscosity, efficient repair of the \cdot TocO radicals by XH9 could well be impeded.^{13,20} These rate constant differences are probably due not only to contrasts in micelle viscosity which governs rates of molecular collision—the TX100 interior being significantly more viscous than that of CTAB²¹—but also due to contrasts in electrostatic character which can also direct the mean location of solubilised reactants. In the uncharged TX100 micelle, it cannot be excluded that the rather small \cdot TocO radical repair by XH9 may be due to a H-atom transfer. Examination of these data taken all together shows that the repair efficiency of the α -tocopheroxyl radical by XH9 is strongly dependent on the micro-environment in which both XH9 and TocOH are located. The efficiency of \cdot TocO radical repair by ascorbate has also been shown to depend notably on the medium.¹⁸

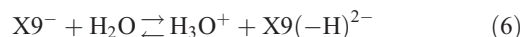
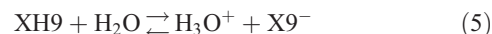
Studies in basic aqueous solutions

In micelles parameters such as polarity, dielectric constant and proton activity vary significantly in different regions of the

particle. Hence, electron transfer involving TocOH, TrOH and XH9 in micellar media does not allow one to obtain thermodynamic data on electron transfer which can be readily interpreted. This limitation applies to the transfer rate dependence on pH or determination of the pK_a for the equilibrium between the ionic species and \cdot X9 radicals involved. Finally, it cannot give access to the reduction potential of the [\cdot X9, H^+ /XH9] couple. The above study in micelles suggests that this potential must be lower than that of the [\cdot TocO, H^+ /TocOH] couple (480 mV at pH7) but higher than that of the [$A^{\cdot-}$, H^+ /AH $^-$] couple (~ 280 mV)⁸ since the latter repairs the \cdot X9 radicals. To overcome solubility problems in such measurements with XH9, the radical behaviour has been further studied in basic solutions.

Ionic equilibria involving XH9 in aqueous solutions

Fig. 4 shows the absorbance spectra of XH9 at pH 7 and under two relevant alkaline pH conditions. A titration graph has been constructed from data taken at 420 nm (insert Fig. 4). The highest pH for which measurements were made is pH 11.9 since XH9 rapidly auto-oxidizes at higher values (data not shown). As the molecule contains 4 hydroxyl groups, two pK_a values have been determined reflecting two equilibria,



A fit of the experimental data assuming these equilibria yields $pK_{a1} = 9.55$ and $pK_{a2} = 11.05$, and molar extinction coefficients of 1050, 7000 and 8250 $M^{-1} cm^{-1}$ at 420 nm for XH9, $X9^-$ and $X9(-H)^{2-}$, respectively. The appropriateness of the fit is demonstrated by the calculated value of 1050 $M^{-1} cm^{-1}$ for the molar extinction coefficient of the unionized species at 420 nm, in

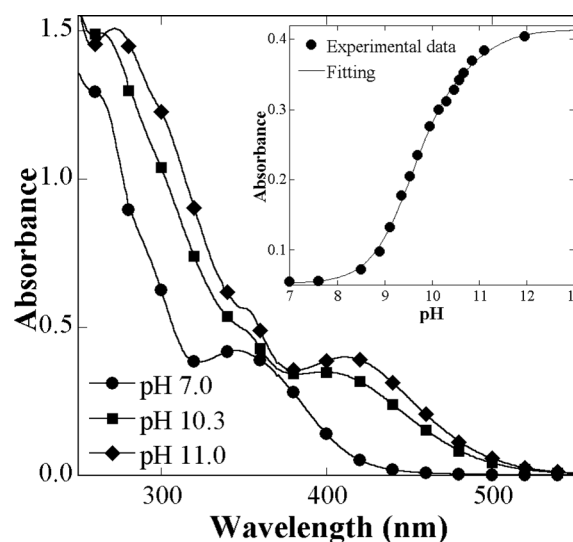


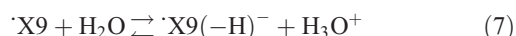
Fig. 4 Absorbance spectra of 50 μ M XH9 (light path: 1 cm) under different pH conditions in air-saturated solutions at 22 $^{\circ}C$ (see text). **Insert:** experimental and calculated absorbance at 420 nm as a function of pH. The calculation was performed assuming the equilibrium between neutral and ionized species as described in the text.

excellent agreement with the experimental value deduced from Fig. 4.

Determination of the pK_a of the $\cdot X9$ radical

The one-electron oxidation of XH9 by $\cdot Br_2^-$ has been measured in neutral or alkaline aqueous solutions. The transient absorbance of the $\cdot X9$ radicals at pH 7 is already known from previous studies.⁶ The transient spectrum from the deprotonated radical species obtained 100 μs and 20 ms after pulse radiolysis at pH 11 is shown on Fig. 5A.

It can be deduced that these initial radicals react further to generate product(s). This transformation occurs within 15–20 ms (data not shown). In view of the spectral shape of the $\cdot X9$ transient at both neutral and alkaline pH and given its time evolution in alkaline solutions, the pH dependence of the $\cdot X9$ transient absorbance was measured at 550 nm, at the end of the oxidation by $\cdot Br_2^-$, e.g. $\sim 100 \mu s$ after the pulse. At that time, it may be assumed that the absorbance of the transient species is that of the one-electron oxidation product of XH9 or its ionized analog, according to the ionic equilibrium:



The pH dependence of the transient absorbance, shown in the insert of Fig. 5A, suggests that the pK_a of the $\cdot X9$ radical (pK_a) is ~ 10 given the experimental uncertainty of data above pH 11.

Estimate of the reduction potential of the $\cdot X9$ radical

A quantitative measure of the electron donating capacity of XH9 is expressed by its one-electron reduction potential. Methods for measuring unknown reduction potentials as well as their limitations have been extensively reported.^{8,22,23} In principle, if an equilibrium is observed during electron transfer processes such as those described above with $\cdot TrO$ and XH9, or $\cdot X9$ and AH^- —and before the radicals decay by other processes—it is possible to determine the associated equilibrium constant (K).

From this parameter, the redox potential may be obtained using the Nernst equation: $R T \ln K = n F \Delta E_0^\circ$, where $R = 8.31 \text{ J K}^{-1} \text{ mol}^{-1}$, $F = 9.65 \times 10^4 \text{ C mol}^{-1}$, T is the absolute temperature ($^\circ\text{K}$) and ΔE_0° is the difference in the redox potential (V) between the two couples involved in the electron transfer. The determination of the reduction potential of the $[\cdot X9, H^+/XH9]$ couple may be performed with either standard used in this study, namely $\cdot TrOH$ or ascorbate. However, two limitations are encountered. First, the ascorbate radical absorbs negligibly above 400 nm, where the LED light source can be used for monitoring transient behavior. Secondly, the $\cdot X9$ radical decomposes over 15–20 ms as shown in Fig. 5A and 5B. Consequently, the reduction potential of the $[\cdot X9, H^+/XH9]$ couple was estimated using $\cdot TrOH$ as the standard. The $\cdot TrO$ radical is produced at a high yield ($\sim 0.6 \mu\text{M Gy}^{-1}$ at pH 11) upon reaction of 2.5 mM $\cdot TrOH$ with $\cdot Br_2^-$ (Fig. 5B). This radical absorbs maximally at 430 nm, a wavelength of very low absorbance for the $\cdot X9$ radical and associated product(s). A concentration of $7 \mu\text{M}$ $\cdot TrO$ was produced by a dose of 14 Gy. Fig. 5B shows the time dependence of the $\cdot TrO$ radical in the absence and in the

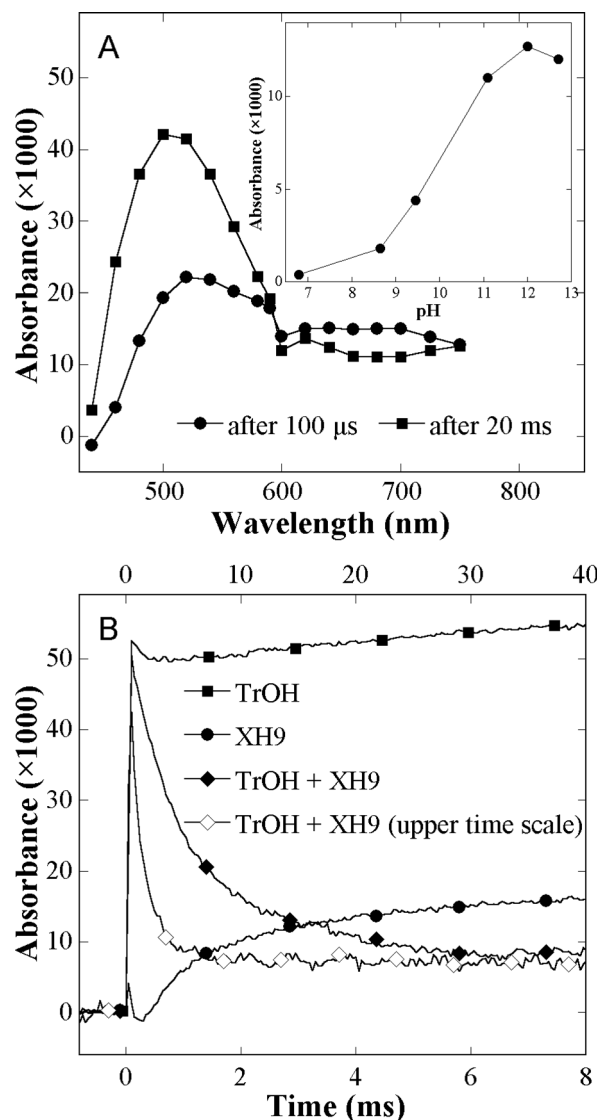
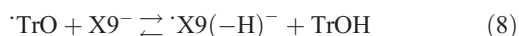


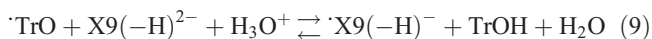
Fig. 5 A. Transient absorbance spectra obtained 100 μs (●) and 20 ms (■) after pulse radiolysis of N_2O -saturated, pH 11 aqueous solutions containing 0.1 M KBr and 200 μM XH9. Dose was 14.2 Gy. **Insert:** pH dependence of the 550 nm transient absorbance measured 100 μs after pulse under the same dose conditions as above but $[XH9] = 50 \mu M$. **B.** Time dependence of 430 nm transient absorbance obtained after pulse radiolysis of N_2O -saturated, pH 11 aqueous solutions containing 0.1 M KBr and 2.5 mM $\cdot TrOH$ (■) or 100 μM XH9 (●) or their mixture at the same concentrations (◆, ◇). Dose was 14.2 Gy in all cases. Note that the decay shown on a longer time scale (upper time scale, symbol ◇ for the graph) is the same as (◆) but on an extended scale. This illustrates the rather stable transient absorbance of $\cdot TrO$ radical up to 40 ms in the presence of 100 μM XH9.

presence of 100 μM XH9 at pH 11. The low $[XH9]$ and the high $[TrOH]$ preclude significant direct oxidation of XH9 by $\cdot Br_2^-$. It may be seen that repair of $\cdot TrO$ is slow, occurring with a rate constant of $1.1 \times 10^3 \text{ M}^{-1} \text{ s}^{-1}$. A $\cdot TrO$ concentration of 1.1 μM is still present 8 ms after the radiolytic pulse with no further change up to 40 ms, suggesting that the repair reaction is incomplete.

To explain the plateau value, it may tentatively be assumed that the following equilibria take place:



and



leading to an equilibrium constant $K \sim 130$. This value is calculated from the $\cdot\text{TrO}$ concentration obtained at equilibrium (1.1 μM , see above) which yields a $\cdot\text{X9}(-\text{H})^-$ concentration of 5.9 μM at equilibrium. Consequently, the ΔE° of the one-electron reduction potential for the two couples together, [$\cdot\text{X9}, \text{H}^+/\text{XH9}$] and [$\cdot\text{TrO}, \text{H}^+/\text{TrOH}$], at pH 11 can be estimated to be ~ 120 mV. The reduction potential of the [$\cdot\text{TrO}, \text{H}^+/\text{TrOH}$] couple at pH 11 (E_{11}°), with reference to the normal hydrogen electrode (NHE), has been previously reported to be ~ 250 mV⁸. As a result, it may be estimated that E_{11}° [$\cdot\text{X9}, \text{H}^+/\text{XH9}$] ~ 130 mV. This value is in good agreement with that obtained by cyclic voltammetry at pH 11, *i.e.* 100 mV vs. NHE and shown below.

Cyclic voltammetry of XH9 at pH 11

Cyclic voltammetry is the method of choice to confirm independently the redox potential of XH9 at pH 11. The measured voltammograms show two oxidation and one reduction peaks (Fig. 6A). The current intensity related to the first oxidation peak is found to be proportional to the XH9 concentration while that of the second oxidation peak increases disproportionately with the three XH9 concentrations used (0.1, 0.2 and 0.5 mM; data not shown). This may be explained by adsorption phenomena or by formation of secondary species that impede further oxidation. The reduction peak is much smaller than the two oxidation peaks and its current intensity is not proportional to the XH9 concentration. Upon inverting the potential before reaching the second oxidation peak, the current intensity remains proportional to the XH9 concentration but that related to the reduction peak becomes proportional to the XH9 concentration.

Knowledge of the reduction potential of radicals—resulting from the one-electron oxidation of hydrophobic polyphenolic antioxidants at alkaline pH—is necessary to calculate the standard redox potential at pH 7 (E_7°) using the equation originally derived by Ilan *et al.*²⁴ This equation may be written as: $E_{11}^\circ = E_0^\circ + 0.059 \log\{K_{a1}K_{a2} + K_{a1}[\text{H}^+] + [\text{H}^+]^2/(K_{a1} + [\text{H}^+])\}$. This equation has been applied to flavonoids⁸ and other phenoxyl radicals.^{9,23} In the case of the [$\cdot\text{X9}, \text{H}^+/\text{XH9}$] couple—where K_{a1} , K_{a2} and K_a are respectively the $\text{p}K_a$ of the mono- and di-anions of XH9 and of the $\cdot\text{X9}$ radical—this equation yields values of 730 and 315 mV for E_0° and E_7° respectively. The E_7° value is notably lower than that of the [$\cdot\text{TrO}, \text{H}^+/\text{TrOH}$] couple but higher than that of the [$\cdot\text{A}^-, \text{H}^+/\text{AH}^-$] couple (~ 280 mV).

For the purpose of comparison, Fig. 6B shows the variation of the redox potential of the species present in the solution for XH9. Cyclic voltammetry measurements yield values of 170 mV and 470 mV at pH 7.4 and pH 4, respectively, in reasonable agreement with the theoretical graph. Similar data were obtained with TrOH by Jovanovic *et al.*⁸ These data are consistent with the electron transfer from XH9 to the $\cdot\text{TrO}$ and $\cdot\text{TocO}$ radicals and the repair of $\cdot\text{X9}$ by ascorbate in neutral solutions. Direct

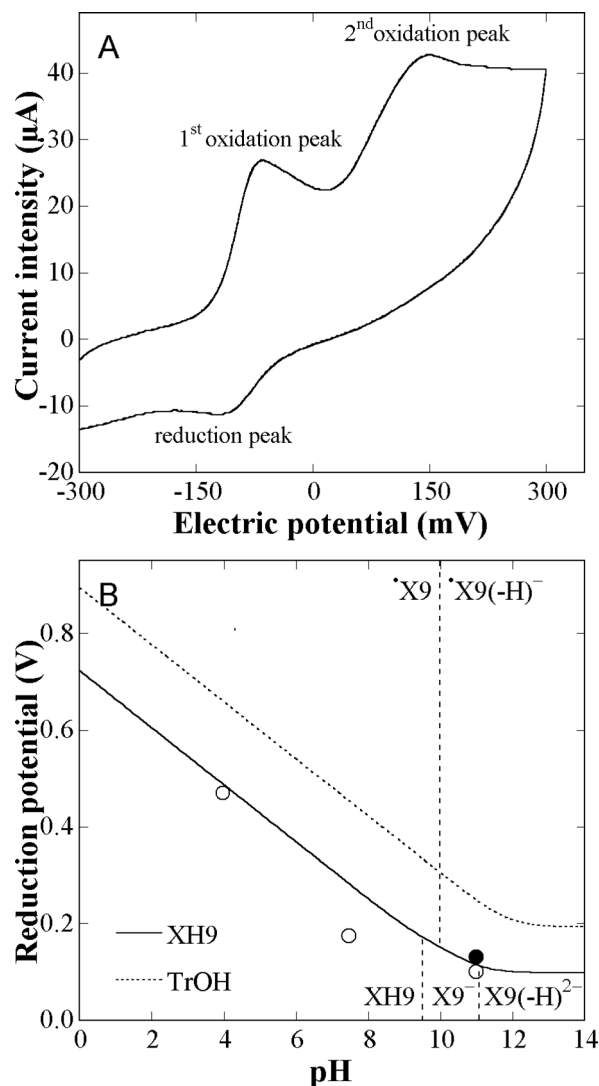


Fig. 6 A. Cyclic voltammogram of 0.1 mM XH9 in pH 11 carbonate buffer versus Ag/AgCl. Scan rate was 100 mV s⁻¹. B. Calculated pH dependence of the redox potentials of XH9 and TrOH and corresponding ionic and redox species associated with XH9. The experimental results for XH9 obtained by pulse radiolysis and cyclic voltammetry are shown by (●) and (○), respectively. Calculation has been performed using their average value at pH 11. The graph for TrOH is taken from ref. 8.

measurements in neutral solutions cannot be performed because of the rather low solubility of the XH and because our data obtained with the micelles suggest that electron transfer processes are slow.

Concluding remarks

A representative member of the hydroxy-2,3-diarylxanthenes, namely, 2,3-bis(3,4-dihydroxyphenyl)-9H-xanthen-9-one (XH9) reduces $\cdot\text{TocO}$, but the repair depends strongly on micro-environment. The other XH do not repair $\cdot\text{TrO}$ and $\cdot\text{TocO}$ radicals, most probably because of a deeper location in the micelles. The regeneration of α -tocopherol, observed here with XH9, has been also observed with other antioxidants including a few

members of the flavonoid family. Indeed quercetin, whose one-electron reduction potential ($E_7^{\circ} = 0.33$ V) is slightly higher than that of the $\cdot\text{X9}, \text{H}^+/\text{XH9}$ couple, also repairs the $\cdot\text{TocO}$ radical.⁸ However, XH9 is much more effective than quercetin in protecting human LDL and cultured human skin keratinocytes from oxidative stresses.⁶ Moreover, other XH of this study, such as XH3 whose standard redox potential is rather similar to that of quercetin, do not repair the $\cdot\text{TrO}$ and $\cdot\text{TocO}$ radicals but are much more effective than XH9 in inhibiting human LDL lipid peroxidation. Thus, the combination of the previous data with those of the present study strongly supports the contention that not only thermodynamic parameters but also hydrophobic character and structural factors play a determining role in the XH antioxidant activity.⁶

Acknowledgements

This work was supported by the Franco-Portuguese exchange programs Pessoa 07958NF. Thanks are due to the Faculdade de Farmácia da Universidade do Porto, and also to University of Aveiro, to the Portuguese Foundation for Science and Technology (FCT) and FEDER for funding the Organic Chemistry Research Unit and the Portuguese National NMR Network.

References

- 1 L. Gales and A. M. Damas, *Curr. Med. Chem.*, 2005, **12**, 2499–2515.
- 2 H. Z. Zhang, S. Kasibhatla, Y. Wang, J. Herich, J. Guastella, B. Tseng, J. Drewe and S. X. Cai, *Bioorg. Med. Chem.*, 2004, **12**, 309–317.
- 3 A. E. Hay, M. C. Aumond, S. Mallet, V. Dumontet, M. Litaudon, D. Rondeau and P. Richomme, *J. Nat. Prod.*, 2004, **67**, 707–709.
- 4 C. M. M. Santos, A. M. S. Silva and J. A. S. Cavaleiro, *Eur. J. Org. Chem.*, 2009, **16**, 2642–2660.
- 5 C. M. M. Santos, M. Freitas, D. Ribeiro, A. Gomes, A. M. S. Silva, J. A. S. Cavaleiro and E. Fernandes, *Bioorg. Med. Chem.*, 2010, **18**, 6776–6784.
- 6 C. M. M. Santos, A. M. S. Silva, P. Filipe, R. Santus, L. K. Patterson, J.-C. Mazière, J. A. Cavaleiro and P. Morlière, *Org. Biomol. Chem.*, 2011, **9**, 3965–3974.
- 7 T. Motoyama, M. Miki, M. Mino, M. Takahashi and E. Niki, *Arch. Biochem. Biophys.*, 1989, **270**, 655–661.
- 8 S. V. Jovanovic, S. Steenken, Y. Hara and M. G. Simic, *J. Chem. Soc., Perkin Trans. 2*, 1996, 2497–2504.
- 9 S. Steenken and P. Neta, *J. Phys. Chem.*, 1982, **86**, 3661–3667.
- 10 L. K. Patterson and J. A. Lilie, *Int. J. Radiat. Phys. Chem.*, 1974, **6**, 129–141.
- 11 G. L. Hug, Y. Wang, C. Schoneich, P. Y. Jiang and R. W. Fessenden, *Radiat. Phys. Chem.*, 1999, **54**, 559–566.
- 12 R. H. Schuler, L. K. Patterson and E. Janata, *J. Phys. Chem.*, 1980, **84**, 2088–2089.
- 13 A. M. S. Silva, P. Filipe, R. S. G. R. Seixas, D. C. G. A. Pinto, L. K. Patterson, G. L. Hug, J. A. S. Cavaleiro, J.-C. Mazière, R. Santus and P. Morlière, *J. Phys. Chem. B*, 2008, **112**, 11456–11461.
- 14 M. J. Davies, L. G. Forni and R. L. Wilson, *Biochem. J.*, 1988, **255**, 513–522.
- 15 T. Proske and A. Henglein, *Ber. Bunsenges. Phys. Chem.*, 1978, **82**, 711–713.
- 16 R. Amorati, F. Ferroni, G. F. Pedulli and L. Valgimigli, *J. Org. Chem.*, 2003, **68**, 9654–9658.
- 17 J. J. Warren and J. M. Mayer, *J. Am. Chem. Soc.*, 2008, **130**, 7546–754718.
- 18 R. H. Bisby and A. W. Parker, *FEBS Lett.*, 1991, **290**, 205–208.
- 19 L. K. Patterson and E. Vieil, *J. Phys. Chem.*, 1973, **77**, 1191–1192.
- 20 D. Panda, S. Khatua and A. Datta, *J. Phys. Chem. B*, 2007, **111**, 1648–1656.
- 21 K. Kano, Y. Ueno and S. Hashimoto, *J. Phys. Chem.*, 1985, **89**, 3161–3166.
- 22 L. G. Forni and R. L. Willson, *Methods Enzymol.*, 1984, **105**, 179–188.
- 23 S. Steenken and P. Neta, *J. Phys. Chem.*, 1979, **83**, 1134–1137.
- 24 W. A. Ilan, G. Czapski and D. Meisel, *Biochim. Biophys. Acta*, 1976, **430**, 209–224.